Journal of Advanced Research in Applied Sciences and Engineering Technology

Journal homepage:
https://semarakilmu.com.my/journals/index.php/applied_sciences_eng_tech/index
ISSN: 2462-1943

Development of Second Order High Frequency Filter for Partial Discharge Measurement

Syed Akhmal Syed Jamalil[1,2*], Zalikha Shamsul[1], Muzamir Isa[1,2], Ahmad Zaidi Abdullah[1,2], Ayob Nazmi Nanyan[1,2]

[1] Faculty of Electrical Engineering & Technology, Universiti Malaysia Perlis , Malayisa
[2] UniMAP High Voltage Transient and Insulation Health Research Group (HVTrans), Perlis, Malaysia

ARTICLE INFO

Article history:
Received 17 August 2023
Received in revised form 7 November 2023
Accepted 19 December 2023
Available online 20 March 2024

Keywords:
Partial Discharge (PD), Sallen-Key, High Pass Filter (HPF), Interference Noise, Cut-off Frequency

ABSTRACT

Partial Discharge (PD) can occur on any high-voltage equipment. This study is particularly concerned with the PD that occurs on underground cables. Researchers frequently struggle to isolate interference noise from the PD signal when doing PD measurements. Therefore, to reduce the interference noise during PD measurements, Sallen-Key High Pass Filter (HPF) with a 500 kHz, or a little bit higher cut-off frequency are designed. This filter is designed with a designated cut-off frequency value because the frequency range of the PD signal is between 1 MHz to 1 GHz. Based on the results of experimental testing for actual filters, the designed filter is a HPF with a cut-off frequency of 500 kHz. When the generator function's input frequency values are set between 500 kHz and 2.4 MHz, the signal will pass the filter and provide output values for both frequencies and amplitude. However, at frequencies lower than 500 kHz, the signal is beginning to be filtered and the output signal's amplitude is getting close to zero. Based on the PD testing results, there is interference on the PD signal shown on the oscilloscope when a 1kV supply is applied to an underground cable without using a filter. But, when the proposed filter is used in PD testing, the ripple voltage is reduced from 123 mV to 67 mV. This proves that when the designed HPF is used in PD testing, it can reduce interference noise on the PD signal.

1. Introduction

According to International Electro-technical Commission (IEC) standard 60270, PD is a localized electrical discharge that incompletely bridges the insulation between conductors. PD is the cause of insulation damage to power equipment [1,2]. It occurs when there is an electrical spark that results when the insulation is open or damaged. This will cause a defect in the power equipment [3,4]. The variation in PD is caused by the electrical breakdown that emerges from the cavity within the insulator [5,6]. Based on the studies by Li *et al*., [7] the operating frequency of power systems depends on the insulation quality of power cables. Many projects demonstrated that the

* *Corresponding author.*
E-mail address: syedakhmal@unimap.edu.my

https://doi.org/10.37934/araset.41.2.194207

measurement of PD is a reliable way to assess the cable's status [8-11]. However, there may be numerous active PD sources detected at once in a real power system, raising the possibility that PD sources are misclassified and interpreted incorrectly [12-14]. Therefore, a device or set of tools is required to distinguish the PD signal to ensure that it is the right PD signal. In relation to research by Bohari *et al.,* [14] the internal discharge current resembles a narrow impulse in shape, with a rapid rising time and an extended tail. Generally, the shapes of PD pulses imply composite pulses, which may be a sign of several PD events occurring within the void region [16,17].

The characteristics of the filters applied in PD measurement allow the current pulse signals to be integrated to produce a pulse magnitude that is proportional to the charge in the PD pulse. Common PD pulse detectors have some limitations in that they may react inaccurately to various PD types [18-20]. According to Rodrigo *et al.,* [21] common measuring quantities, such as the peak value of the detected PD pulse by semi-integration, can give misleading results due to repeated PD occurrences in a void within High Voltage (HV) Cables.

Based on studies by Dey *et.al.,* [22], in general, electrical measures, which are PD signals that are acquired in the form of individual or series of electrical pulses, are the most widely used in PD detection technology. One of the most difficult tasks, especially in online systems, is separating PD pulses from noise. Corresponding to Nagashan *et. al.,* [23] one of the most crucial problems that PD signals must tackle is unwanted signal noise.

Based on studies many researchers have investigated various detection techniques, such as pulse current method, ultrasonic method, ultra high frequency (UHF) method, optical measurement method, etc [24-25]. However, the filters employed in the detection method frequently do not use HPF as the signal's filtering component, and in some instances, they do not use any filters at all. Many projects on PD detection techniques use passive filters and Low Pass Filters (LPF) as their signal filtering components. Radzi *et al.,* [26] research on PD detection on medium voltage Cross-Linked Polyethylene (XLPE) cable used band pass filters. Neha *et al.,* [27] research on PD detection technique on exposed XLPE Cables to Lightning Impulse voltage have used passive filters.

Low-noise PD signals must be isolated and limited in frequency using the HPF developed for this study [28,29]. Since the data analysis software can integrate with the active component on the HPF and transform it into data for additional analysis, HPF as an active filter may also be implemented as the digital component. This study will make use of the Sallen-Key HPF technique to improve the precision of PD signal measurement. As recommended and described in this work, the HPF is essential for identifying high-frequency electromagnetic signals, particularly in faulty HV cables.

With this study, a novel method of signal filtering was established that was distinct from the conventional filter previously applied to measurements. This particular HPF will eliminate unwanted noise, improve certain frequency band, or isolate a particular signal. The second order Butterworth HPF effectively achieves this noise reduction without distorting the signal excessively. The project also considers how different parts or circuits interact with one another, such as through feedback, distortion, phase shift, or interference. To enhance the performance and quality of the signals detected which incorporated with the newly developed Printed Circuit Board (PCB) sensors.

2. Methodology

2.1 High Pass Filter (HPF) Development

The selection of the operational amplifier is the most crucial stage in creating a well-fitting design for the project, followed by considering about the right sort of filter to use. The selection of the operational amplifier is the most crucial stage in creating a well-fitting design for the project, followed by considering about the right sort of filter to use. An active filter integrating a high-frequency op-

amp and a Sallen-Key Butterworth HPF design is ideal for this task. Considering the selection of the appropriate filter type, the filter's op-amp must be well selected in order to obtain the high value of the cut-off frequency. Sallen Key filters offer a simple and effective solution for implementing a wide range of filter types in electronic circuits. The Sallen Key HPF consists of an op-amp and two capacitors and two resistors in a specific configuration. The input signal is applied to the non-inverting input of the op-amp, while the output signal is taken from the output of the op-amp. The two capacitors and two resistors create a frequency-dependent response that attenuates signals below the cutoff frequency while allowing signals above the cutoff frequency to pass through. For this particular HPF design, the cut-off frequency is set to 500 kHz. The procedure will start with simulation testing employing the op-amp MAX4412 because it has a really high frequency of 500MHz -3dB while only requiring 1.7mA of supply current per amplifier. The design will then be transformed to PCB development for testing in functional and performance tests.

2.2 Butterworth Filter Design Selection

A Butterworth filter is a type of electronic filter that has a flat frequency response in the passband and rolls off smoothly in the stopband. It is a popular choice for applications that require a smooth frequency response, such as audio processing and data communication. To design the HPF, the calculation will be based on a Butterworth filter table which provide references on the coefficients or parameters for designing a Butterworth filter. The Butterworth filter table typically includes the filter order, cut-off frequency, and the corresponding coefficients for the filter transfer function. The filter order refers to the degree of the polynomial in the transfer function, which determines the steepness of the filter's roll-off. The cut-off frequency is the frequency at which the filter starts to attenuate the signal. The coefficients are used to calculate the filter response based on the input signal frequency. Table 1 shows the Butterworth filter table that has been used for this filter design.

Table 1
Butterworth Filter Table

FILTER ORDER	Stage 1		Stage 2		Stage 3		Stage 4		Stage 5	
	FSF	Q	FSF	Q	FSF	Q	FSF	Q	FSF	Q
2	1.000	0.7071								
3	1.000	1.000	1.000							
4	1.000	0.5412	1.000	1.3065						
5	1.000	0.6180	1.000	1.6181	1.000					
6	1.000	0.5177	1.000	0.7071	1.000	1.9320				
7	1.000	0.5549	1.000	0.8019	1.000	2.2472	1.000			
8	1.000	0.5098	1.000	0.6013	1.000	0.8999	1.000	2.5628		
9	1.000	0.5321	1.000	0.6527	1.000	1.000	1.000	2.8802	1.000	
10	1.000	0.5062	1.000	0.5612	1.000	0.7071	1.000	1.1013	1.000	3.1969

2.3 Sallen Key Butterworth HPF Design Calculation

For this HPF, since gain is equal to 1 (voltage follower), the ratio value for the filter component is 0. This part consists of Sallen-Key design simplification for a Sallen-Key Butterworth HPF with unity gain. For HPF design, the cut-off frequency is set to 500 kHz. R and C were assumed as the following formula:

$R_A = R$, $R_B = mR$, $C_A = nC$ and $C_B = C$

Therefore, the critical frequency of the HPF will be as in Eq. (1),

$$f_C = \frac{1}{2\pi RC\sqrt{mn}} \tag{1}$$

and the value Q is determined by filter component ratio the formula for Q_{HP} is shown as follows as in Eq. (2),

$$Q_{HP} = \frac{\sqrt{mn}}{1+n} \tag{2}$$

This part consists of the Sallen-Key Butterworth HPF Design Calculation that will be used for filter design. It also included the formula used for the HPF design.

Stage 1: 2nd order

Assume, $n = 5$ for $Q_{HP} = \frac{\sqrt{mn}}{1+n}$. The value of Q can be referred to Butterworth filter based on filter stage.

$Q_{HP} = \frac{\sqrt{5m}}{1+n} = 0.5412$ then will result $m = 2.109$ and assume $C_{B1} = C = 22pF$ and $fc = 500kHz$

So, from $R_{A1} = R = \frac{1}{2\pi Cfc\sqrt{mn}}$, the equation will produce $R_{A1} = 4.42k\Omega$, $R_{B1} = mR = 9.32k\Omega$ and $C_{A1} = nC = 110pF$

Stage 2: 4th order

Using the same equation $Q_{HP} = \frac{\sqrt{mn}}{1+n}$ with the value Q referred to the Butterworth Filter table will result in $m = 12.29$ and the rest of the component values.

$C_{B2} = C = 22pF$, $R_{A2} = 1.82k\Omega$, $R_{B2} = 22.1k\Omega$ and $C_{A2} = 110pF$

2.4 HPF Design Simulation

Proteus 8 Professional software will be used to simulate the HPF design first as in Fig. 1. Based on the previous calculations, the HPF value will be determined. The Sallen Key Butterworth HPF will serve as guidelines for the design's setup. On the simulation procedure, a high-frequency op-amp (MAX4412EUK-T) will be used. The op-amp will operate at +4.5V to +11V, hence a source of +5V must be added in order to activate the HPF. Fig. 1 shows the simulation design of the Sallen Key Butterworth HPF. The buffer circuit is connected at the first stage of HPF design to prevent the frequency response curve from being affected. The buffer is particularly beneficial because it prevents the input impedance of one stage from loading the output impedance of the previous stage, resulting in signal loss.

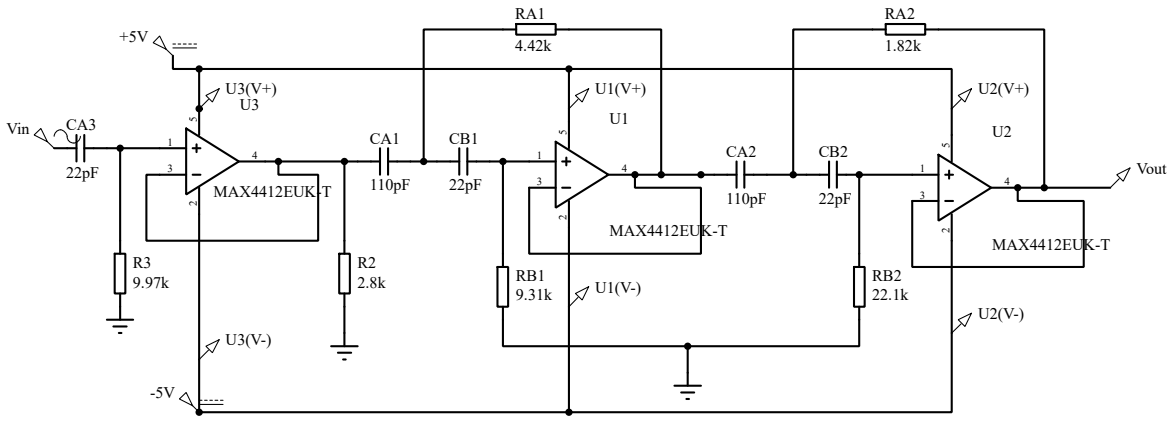

Fig. 1.Simulation Design of sallen key butterworth HPF using proteus software

2.5 HPF PCB Development

Based on the simulation that has been successfully tested, the HPF PCB will be created. The value for PCB design is the same as for simulation. This needs to be considered to ensure that the process for PD measurement can achieve its objective. The PCB design is accomplished with the open-source PCB-making software EasyEDA. Figure 2 shows the schematic for HPF circuit design using EasyEDA. After that, the filter schematic needs to be converted to a PCB. Before fabricating the PCB, the circuit connection must be thoroughly examined. The models of the HPF design are shown in Figure 3 and Figure 4. PCB fabrication offers several advantages over simple wire connections, making it a more reliable choice for electronic devices and circuits. PCB fabrication is a highly automated and controlled process. HPF PCB is produced with consistent precision, ensuring that the circuit components are placed accurately and at the correct distances from each other. In contrast, manual wire connections can introduce variations in terms of wire length, positioning, and solder quality, potentially leading to electrical instability and reliability issues. HPF PCB is designed with carefully laid out traces and ground planes that minimize Electromagnetic Interference (EMI). Proper grounding and shielding techniques can be incorporated into the PCB design to mitigate EMI, which is often a challenge in simple wire connections where electromagnetic noise can easily couple into nearby wires, leading to signal degradation and reliability problems.

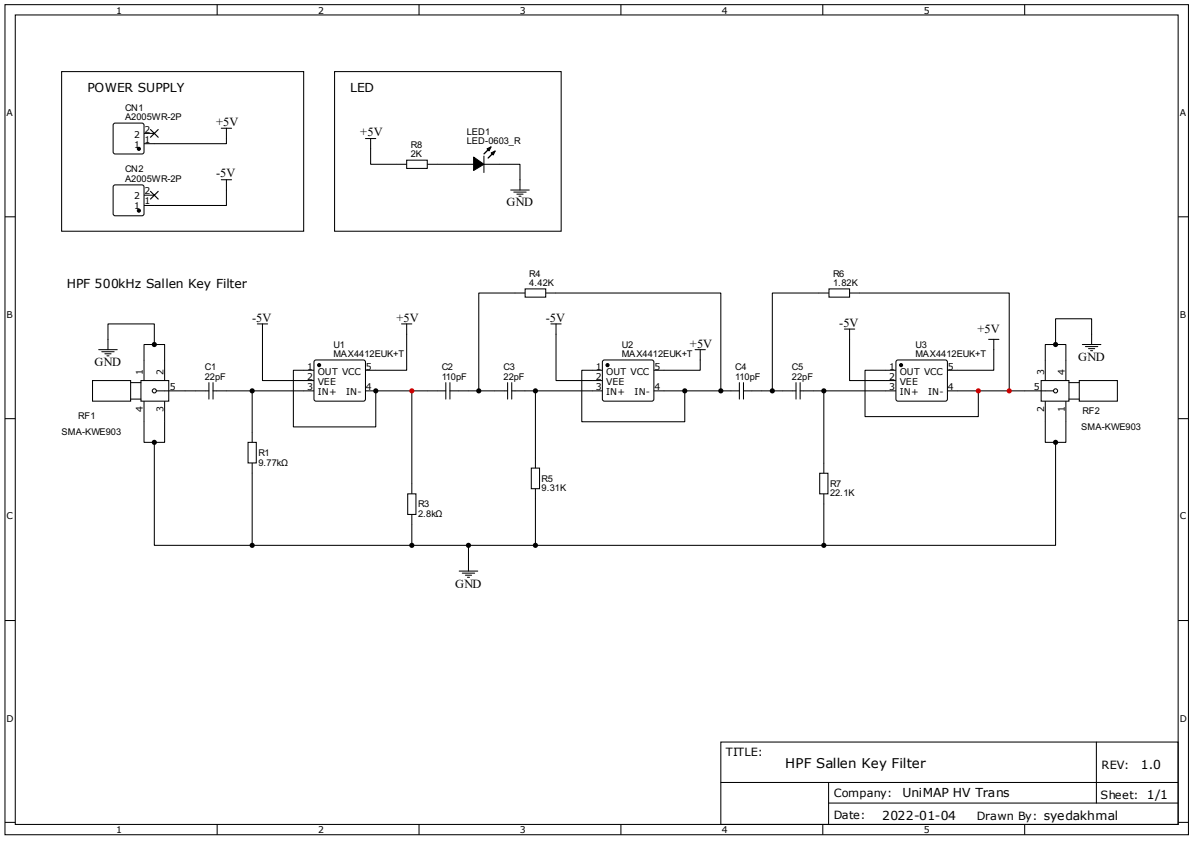

Fig. 2. Schematic circuit design using EasyEDA software

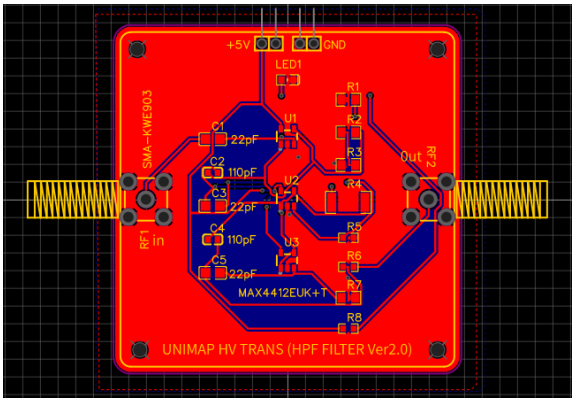

Fig. 3. PCB design using EasyEDA software

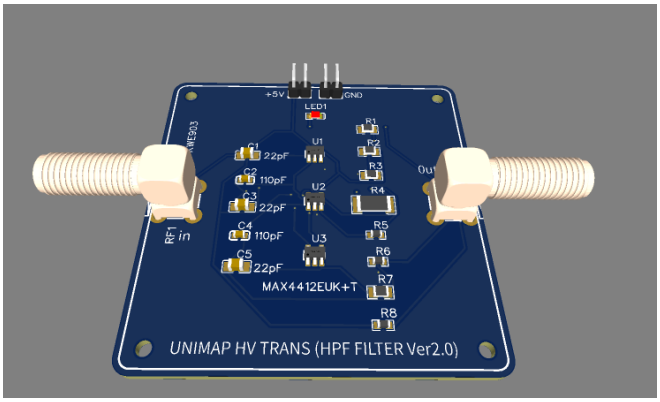

Fig. 4. 3D view of HPF prototype

2.6 PD Measurement Testing Setup

Fig. 5 illustrates the experimental setup for the testing of Partial Discharge (PD) measurement. Parameters for PCB sensors must be calculated and set before the experiment is conducted. Voltage pulses are injected from the Impulse High Voltage Sources using a High Voltage Construction Kit HAEFELY HV test set. Designated PCB sensor is used in this experiment. PCB sensor is connected around the 11kV XLPE cable in the circuit, and it must be grounded. The connection between the PCB sensor and the oscilloscope is made using a Sub Miniature version A (SMA) connector. The output of the PD signal is obtained by connecting the SMA coil terminal using a low-capacitance Active Differential Probe (ADP) to the LeCroy Wavesurfer 24Xs oscilloscope. Due to the air core, the sensitivity of the PCB sensor is low, and care must be taken to guarantee the reliability of the

measured signal. Because ADP decouples the RC from ground, it greatly reduces loop currents and common voltages at the terminals Primary current pulses are measured using HFCT as a reference. Tests are carried out by observing the PD output waveforms and the oscillation frequency with the HPF and without a HPF. HV pulses are supplied through the HV cable ranging from 1kV-10kV. Fig. 6 shows the actual HPF which is used in the measurement and Fig. **7** shows the PCB sensor connected to HPF for the PD measurement.

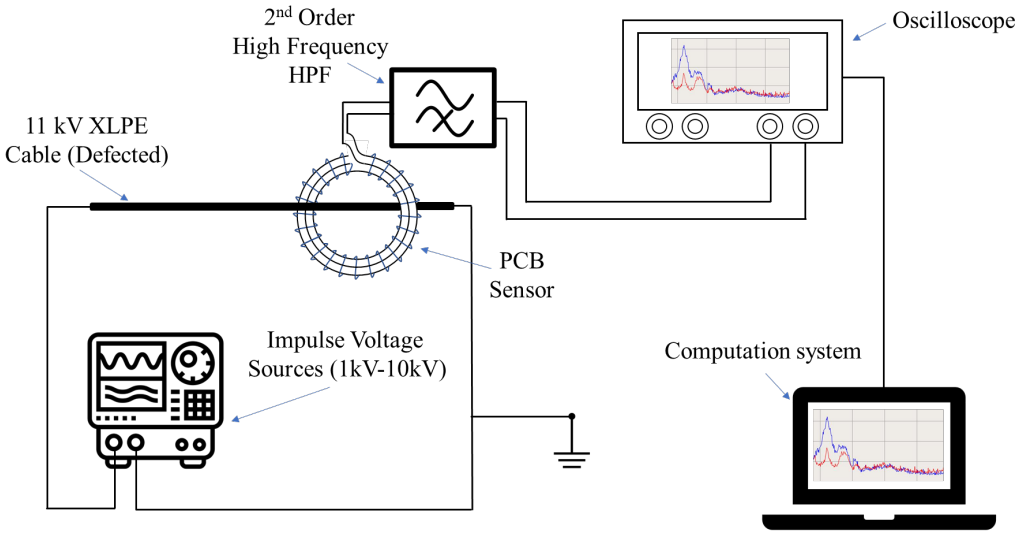

Fig. 5 Experimental setup for partial discharge measurement

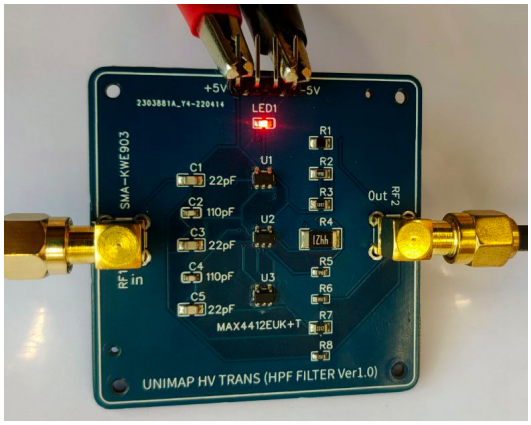

Fig. 6. Second order sallen key HPF PCB prototype

Fig. 7. PCB sensor connected to HPF for PD measurement

3. Result and discussion

This section contains the results of the HPF testing. HPF testing refers to the process of evaluating and assessing the performance and functionality of a high-pass filter in an electronic or signal processing system. A high-pass filter is a type of electronic circuit or digital filter that allows higher-frequency signals to pass through while attenuating or blocking lower-frequency signals. The results comprise two main components of evaluation: simulation-based testing and actual HPF testing. Comparisons will be made between the results of both assessments. The results comprise two main components of evaluation: simulation-based testing and actual HPF testing. Comparisons will be made between the results of both assessments. This simulation is ran using Proteus 8 Professional

and also performing application testing. The application testing is done to prove the effectiveness of the HPF that has been designed for PD measurement.

3.1 Result for filter HPF Functional Testing

Functional testing refers to the process of evaluating and assessing the performance and functionality of the HPF in an electronic or signal processing system. HPF is a type of electronic circuit that allows higher-frequency signals to pass through while attenuating or blocking lower-frequency signals. This part consists of the results for the designed HPF PCB measurement test. For this part, the designated HPF PCB will be tested in the laboratory. This test is important to ensure the value of the cut-off frequency is the same as desired, as already stated in the objective. This lab testing result will be compared to the simulation result to ensure that the value of the cut-off frequency is approaching the value from simulation.

3.2 Frequency Respond Curve

This part consists of the comparison of the frequency response curve of the actual HPF based on the experiment result and the ideal HPF based on the simulation result. The difference in value between the experiment result and the simulation result is due to some factor among them: the connection between the components is not very precise. In addition, the poor condition of the components will also affect the results of the experiment.

3.3 Simulation Result of Sallen Key Butterworth HPF

Fig. 8 shows the simulation result for the Sallen Key Butterworth HPF. The design of this HPF is based on the HPF design calculation. The aim of this simulation is to get a 500 kHz and above cut-off frequency value. The highest value of the cut-off frequency needs to be considered in this project because the frequency range of PD is from 1 MHz to 1 GHz. This means if this HPF is designed with a higher cut-off frequency, the frequencies below the cut-off frequency value will be filtered.

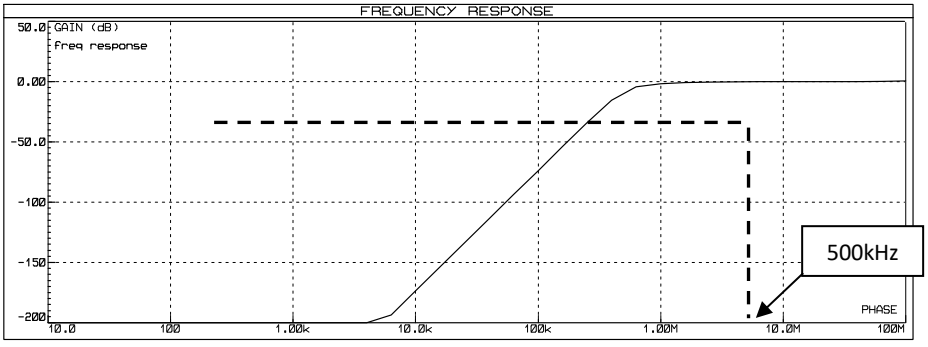

Fig. 8. Frequency response of sallen key butterworth HPF

According to Fig. 8, the simulation of a HPF shows a cutoff frequency of 500 kHz but exhibits a drop in dB at that frequency, it indicates that the HPF is attenuating the signal at the cutoff frequency rather than allowing it to pass through unaffected. This behaviour is expected for a HPF, as it is designed to pass frequencies above the cutoff frequency while attenuating frequencies below it. It's important to note that the drop in dB does not necessarily imply a malfunction or error in the HPF. It

is an inherent characteristic of HPF to attenuate frequencies below the cutoff. However, the magnitude of the drop should align with the expected response based on the HPF design and the range for this HPF design is acceptable in order to capture the PD signal at higher frequency. Since the frequency of PD is high, the HPF design needs to be above 500 kHz. The concept of HPF design is that a HPF will allow signals above the cut-off frequency while filtering signals below it, which are known as interference noise. If a HPF is used in PD measurement, it can effectively filter out the interference noise, increasing the likelihood of detecting a PD signal. Therefore, the simulation results and the cut-off frequency of the HPF are significant in the development of a functional PD measurement system.

3.4 Actual HPF Experiment Result

The result shown for this part is based on the experiment result for an actual HPF. Table 2 shows the actual results of the HPF from a higher to smaller frequencies. The higher frequency that can be setup using a function generator in the lab is 2.4 MHz. In order to get the value of the cut-off frequency, the frequency is decreased until the frequency signal is filtered. Based on the observation, if the frequency is set to 2.4 MHz, the amplitude of the output signal of the HPF is equal to the input signal, which is 0.73V, and the frequency value shows the same as the input frequency, which is 2.4 MHz.

After that, if the frequency is decreased to 1 MHz, the amplitude value of the output signal starts to decrease to 0.7 V, and the frequency value is the same as the input frequency, which is 1 MHz. Next, when the value of frequency is set to 700 kHz, the amplitude value of the output signal is decreased to 0.3 volts, and the frequency signal is started to be filtered, so the frequency value shown is null. This experiment was continued by increasing the frequency value to 450 kHz, while maintaining the amplitude value of the output signal at 0.15V. The frequency signal was also filtered, and the frequency value displayed was null. Finally, the value of frequency is set to 280 kHz and the value of amplitude of the output signal is approaching zero; the amplitude of the output signal shows 0.08V, while the frequency signal remains to be filtered and the frequency value shows is null.

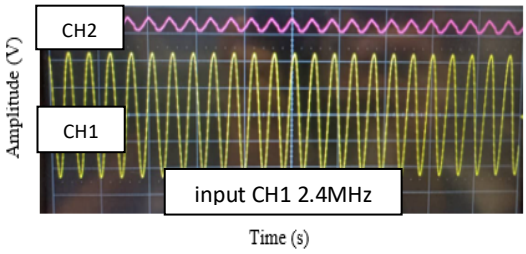

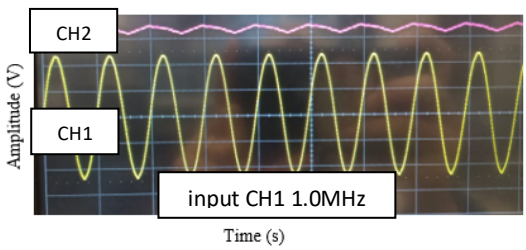

Table 2
Actual HPF experiment result for decreasing from 2.4 MHz to 280 kHz

Measure	Peak to Peak (CH2)	Frequency (CH2)
Value	0.727V	2.363 MHz
Mean	0.731V	2.359 MHz
Min	0.720V	2.339 MHz
Max	0.753V	2.377 MHz
Sdev	0.082V	4.823 kHz
Num	61	671

Measure	Peak to Peak (CH2)	Frequency (CH2)
Value	0.700V	1.003 MHz
Mean	1.6145V	1.861 MHz
Min	0.117V	469.043 kHz
Max	2.45V	3.369 MHz
Sdev	0.672V	396.2 kHz
Num	1950	13702

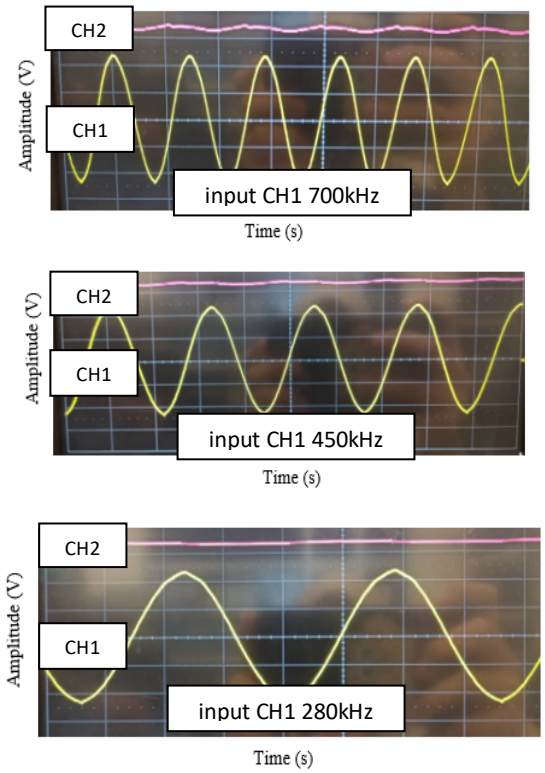

Measure	Peak to Peak (CH2)	Frequency (CH2)
Value	0.267V	---
Mean	1.435V	1.7947 MHz
Min	0.117V	469.043 kHz
Max	2.45V	3.369 MHz
Sdev	0.749V	457.1 kHz
Num	2311	15919

Measure	Peak to Peak (CH2)	Frequency (CH2)
Value	0.150V	---
Mean	1.180V	1.778 MHz
Min	0.117V	450.857 kHz
Max	2.45V	3.369 MHz
Sdev	0.844V	476.6 kHz
Num	2884	16142

Measure	Peak to Peak (CH2)	Frequency (CH2)
Value	0.083V	---
Mean	0.095V	---
Min	0.083V	---
Max	0.150V	---
Sdev	0.018V	---
Num	88	0

Fig. 9. Input and output signals that vary from 2.4 MHz to 280 kHz

3.5 Frequency Responds Curve of Actual HPF

Table 3 shows the amplitude and frequency values for the actual HPF that has been tested in the lab. The value shown is based on the experiment result by the oscilloscope when the frequency values are set from 2.4 MHz to 280 kHz. From the experiment, the frequency curve can be established as shown in Figure 10. The frequency curve's cutoff frequency is around 1 MHz, and the HPF began filtering the signal below that frequency starts from 700 kHz. This is rather higher than the 500 kHz calculated in the simulation, but it is tolerable because there are various factors that cause the two to differ. There may be some loading effects and tolerances in the component. While actual experiments consider the relationships between components in a physical setting, simulations may assume perfect circumstances. To obtain accurate values that match the simulations, there should be some improvement made in the component selection process. The primary goal of this experiment is to cancel out the lower frequency of the signals, so the findings are still acceptable.

3.6 Frequency Responds Curve of Ideal HPF

Table 4 shows the re-plot of the amplitude and frequency value for the designed HPF that has been run using Proteus 8 Professional simulation. Plot point values are derived from simulation results using the same frequency values as the real HPF, which is set between 2.4 MHz and 280 kHz. As previously stated, the behavior is predicted for an HPF as it is intended to pass frequencies beyond the cutoff frequency while attenuating frequencies below it. The findings discovered the same cut off frequency 1 MHz as shown in Figure 11, which is slightly higher than the real determined for the calculation 500 kHz. In fact, the cutoff frequency is the same as it was in the simulation, while the dB level dropped. The important point is that the signal with the lower frequency is cancelled out.

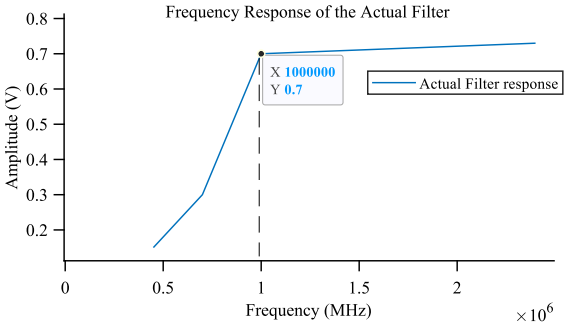

Fig. 10. Frequency response curve of actual HPF

Table 3
Amplitude and frequency value of actual HPF

Amplitude (V)	Frequency (Hz)
0.08	280000
0.15	450000
0.3	700000
0.7	1000000
0.73	2400000

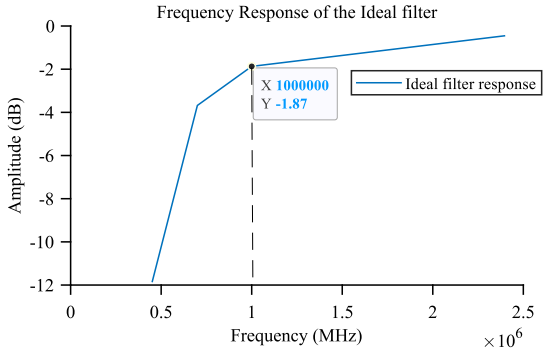

Fig. 11. Frequency response curve of ideal HPF

Table 4
Amplitude and frequency value of ideal HPF

Amplitude (-dB)	Frequency (Hz)
-29.8	280000
-11.87	450000
-3.68	700000
-1.87	1000000
-0.45	2400000

3.7 Result of Application Testing (PD Measurement Test)

This part consists of the PD measurement test result. The result shows the comparison between PD testing without and with the HPF. According to IEC 60060-1 on High Voltage Test Techniques, the minimum applicable test on the dielectric test with direct voltage, alternating voltage, impulse voltage, and combinations of all of them on the HV equipment is 1 kV. And based on international standard IEC 60270, this International Standard is applicable to the measurement of PD which occur in electrical apparatus, components or systems when tested with alternating voltages up to 400 Hz or with direct voltage. However, the measurement test is conducted on a gradually increasing voltage from 1 kV to 10 kV and the result of the minimum voltage test at 1 kV is shown to show the functionality of the designed HPF. PD can occur at relatively low voltage levels, typically starting at voltages above a certain threshold. The specific voltage at which PD begins to appear depends on various factors, including the nature of the insulating material, the geometry of the insulation system, and the presence of impurities or defects. The measurement test was conducted on the 11 kV XLPE cables which require medium voltage for its application. Additionally, the 11 kV XLPE cable is preferred for its many uses, including those that necessitate it to be used indoors, outside, in water, and for its installation underground, all of which involve high mechanical stresses.

3.8 PD Testing Without HPF

For this test, the PCB sensor was connected directly from an underground cable to the oscilloscope. After that, 1 kV of voltage will be supplied to the cable. The signal will be observed using an oscilloscope. Fig. **12** shows the signal for PD testing without using a HPF.

As shown in Fig. **12**, if PD testing is done without using a HPF when 1 kV of voltage is supplied to the cable, it will be seen that there is interference on the PD signal, also called interference noise. This interference noise will make it difficult for engineers to identify the cause of PDs that occur on underground cable. Moreover, if the HPF is not used in the PD testing signal generated to detect PD in the underground cable, it will include all signals, including signals that are not PD signals. This is because with PD signals, the cause of cable damage will be easier to identify.

3.9 PD Testing with HPF

For this test, the designated Sallen-Key HPF will be connected from the PCB sensor to the oscilloscope. 1 kV of voltage will be supplied to the 11 kV XLPE cable. The signal was observed using an oscilloscope. Fig. **13** shows the signal for PD measurement test using the designated HPF. As shown in Fig. **13**, the ripple decreased from 123 mV to 67 mV representing the noise reduction on the output signal. This demonstrates that the HPF implemented in the tests provided the noise cancelling. In addition, the HPF is designed to filter the signal below the cut-off frequency (500 kHz and above). The introduction of the HPF into experiment setup yielded significant improvements in the clarity of the PD signal measurements. Prior to incorporating this HPF, the PD signal was obscured by various noise sources, making it challenging to distinguish and analyse accurately. Upon implementing the designated HPF, it acted as an effective noise-reduction mechanism, selectively attenuating low-frequency noise components while allowing the higher-frequency PD signals to pass through. This selective filtering significantly enhanced the signal's clarity and reduced the influence of unwanted noise sources, such as EMI or background noise. Additionally, this strategic use of the designated HPF gave a substantial enhancement in the signal-to-noise ratio (SNR). Prior to employing the HPF, the noise in the signal was significantly reduced, leading to a notable improvement in the SNR. The data was imported and analysed using the MATLAB software with the signal processing toolbox and the analysis improved with SNR value of 11.3 indicating that the HPF effectively mitigated unwanted noise and enhanced the clarity and reliability of the PD signal measurement.

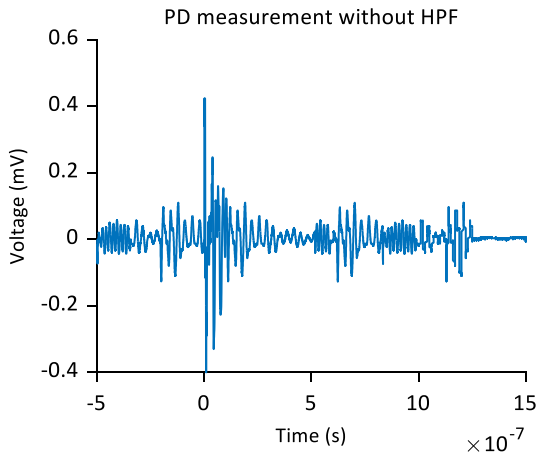

Fig. 12. PD signal without HPF

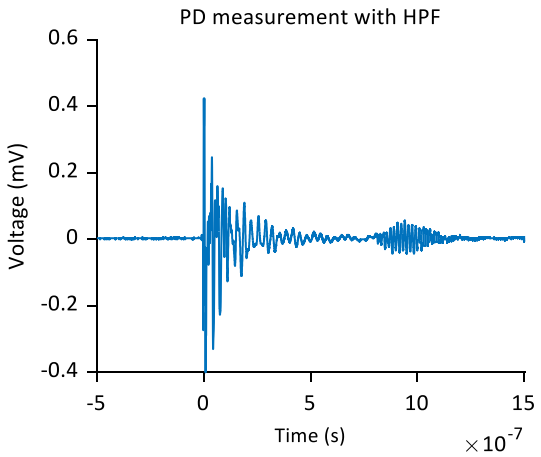

Fig. 13. PD signal with HPF

4. Conclusion

As a conclusion, based on the results, it shows that the HPF is designed to attenuate the lower frequencies and pass the higher frequencies, so the signals are more reliable to be used in PD measurement. Moreover, when the simulation is running by using Proteus 8 Professional for the

Sallen Key Butterworth HPF, the frequency response graph shows a cut-off frequency value of 500 kHz. This can be related to the theory that a HPF will allow signals with a frequency higher than a certain cut-off frequency and attenuate signals with a frequency lower than the cut-off frequency. Based on the experiment results for the actual HPF, the filter design is a HPF with a cut-off frequency of 1 MHz. This is because if the value of frequency is set to its maximum value, which is 2.4 MHz, the value of amplitude and frequency of the output signal are nearly equal to the input signal. After that, if the value of the frequency is decreased starting at 500 kHz, the signal is started to be filtered. For PD measurement results, when PD testing is conducted without filtering, the signal generated to detect a PD signal in the underground cable will include all signals, including non-PD signals. But after the designated HPF is applied for PD testing, the voltage ripple is decreased from 123 mV to 67 mV. This proved that if the designated 2nd order HPF can reduce the unwanted noises in PD testing. The conclusion can be drawn that this HPF is suitable for PD measurement because it will filter the non-PD signal during PD testing. This study presents a novel Butterworth HPF design incorporating a tuneable resonator-based approach, offering improved selectivity and sensitivity for PD measurement focused on the HV cable.

Acknowledgement
This research was not funded by any grant.

References

[1] IEC Standards 60270.(2000). High-voltage test techniques. Partial discharge measurements (IEC 60270:2000). In Bsi (Issue C).
[2] Lemke, Eberhard, Sonja Berlijn, Edward Gulski, Hans Michael Muhr, Edwin Pultrum, Thomas Strehl, Wolfgang Hauschild, Johannes Rickmann, and Guiseppe Rizzi. "Guide for electrical partial discharge measurements in compliance to IEC 60270." Electra 241 (2008): 60-68.
[3] Division, E. W. & I. S. Guideline Measurement and diagnosis of partial discharges in low voltage applications < 1000 volts (p. 23). (2017).
[4] Kinsht, N. V., N. N. Petrunko, N. V. Silin, and S. Y. Tetiora. "To the Issue of the Development of Partial Discharge Theory." In 2019 International Multi-Conference on Industrial Engineering and Modern Technologies (FarEastCon), pp. 1-4. IEEE, 2019. https://doi.org/10.1109/FarEastCon.2019.8934124
[5] Klüss, Joni V., and Alf-Peter Elg. "Challenges associated with implementation of HFCTs for partial discharge measurements." In 2020 Conference on Precision Electromagnetic Measurements (CPEM), pp. 1-2. IEEE, 2020. https://doi.org/10.1109/CPEM49742.2020.9191781
[6] Yousfi, Belkacem, and Ibn Khaldoun Lefkaier. "Simulation of partial discharges initiation in voids in medium voltage cables insulators." IEEE Transactions on Dielectrics and Electrical Insulation 25, no. 3 (2018): 892-899. https://doi.org/10.1109/TDEI.2018.006790
[7] Li, Yufeng, Jinchun Han, Yufeng Du, and Haiyun Jin. "Time–frequency Maps for Multiple Partial Discharge Sources Separation in Cable Terminations." *IEEE Transactions on Power Delivery* (2023). https://doi.org/10.1109/TPWRD.2023.3256127
[8] Chimunda, S., C. Nyamupangedengu, and P. O'Halloran. "Early Detection of Impending Failure in HV Cable Terminations–An Intelligent Asset Management Necessity."
[9] Barbieri, Luca, Andrea Villa, Roberto Malgesini, Daniele Palladini, and Christian Laurano. "An Innovative Sensor for Cable Joint Monitoring and Partial Discharge Localization." Energies 14, no. 14 (2021): 4095. https://doi.org/10.3390/en14144095
[10] Chonpathomphikunloed, W., B. Paophan, A. Kunakorn, P. Yutthagowith, and M. Leelachindakrairerk. "Analyses of Rogowski coils for partial discharge measurement." In 2017 International Symposium on Electrical Insulating Materials (ISEIM), vol. 1, pp. 378-381. IEEE, 2017. https://doi.org/10.23919/ISEIM.2017.8088764
[11] Dwijayatno, Fabianus Marintis, Tessamonica Luthfia, and Nelson Silaen. "Early Warning of XLPE Power Cable Breakdown by Using Partial Discharge Testing." In 2021 3rd International Conference on High Voltage Engineering and Power Systems (ICHVEPS), pp. 558-562. IEEE, 2021. https://doi.org/10.1109/ICHVEPS53178.2021.9600995
[12] Feng, Xianyong, Qing Xiong, Angelo L. Gattozzi, and Robert E. Hebner. "Partial discharge experimental study for medium voltage DC cables." IEEE Transactions on Power Delivery 36, no. 2 (2020): 1128-1136. https://doi.org/10.1109/TPWRD.2020.3002508

[13] Firuzi, Keyvan, and Mehdi Vakilian. "Multi-source partial discharge signals discrimination by six bandpass filters and DBSCAN clustering." In 2018 12th International Conference on the Properties and Applications of Dielectric Materials (ICPADM), pp. 68-71. IEEE, 2018. https://doi.org/10.1109/ICPADM.2018.8401079
[14] Fritz, Jan Niklas, Christoph Neeb, and Rik W. De Doncker. "A PCB integrated differential Rogowski coil for non-intrusive current measurement featuring high bandwidth and dv/dt immunity." (2015): 1-6.
[15] Bohari, Z. H., M. Isa, A. Z. Abdullah, P. J. Soh, M. F. Sulaima, and S. N. M. Arshad. "Performance Assessment for Bare Patch Antenna and Integrated Filter-antenna Microstrip Patch Resonator Based for Partial Discharge Application in HV Equipment." In *2021 8th International Conference on Computer and Communication Engineering (ICCCE)*, pp. 294-298. IEEE, 2021. https://doi.org/10.1109/ICCCE50029.2021.9467215
[16] Tagungsband Zum Power and Energy Student Summit 2015: Dortmund, 13. Und 14. Januar 2015; PESS Dortmund 2015 / Veranst. Vom Institut Für Energiesysteme, Energieeffizienz Und Energiewirtschaft, TU Dortmund. [Konferenzleitung Christian Rehtanz ...], 2, S05.2, 6 Seiten. https://publications.rwth-aachen.de/record/565672
[17] Gao, Angran, Yongli Zhu, Weihao Cai, and Yi Zhang. "Pattern recognition of partial discharge based on VMD-CWD spectrum and optimized CNN with cross-layer feature fusion." Ieee Access 8 (2020): 151296-151306. https://doi.org/10.1109/ACCESS.2020.3017047
[18] Gu, Peng-Yu, Qing Chen, Hong-Bin Li, Chen Hu, Hui Gong, and Yang Jiao. "PCB Rogowski coils for 300 kA current measurement on a multi-split conductor." IEEE Sensors Journal 19, no. 16 (2019): 6786-6794. https://doi.org/10.1109/JSEN.2019.2914730
[19] Han, Ruo-Yu, Jia-Wei Wu, Wei-Dong Ding, Yan Jing, Hai-Bin Zhou, Qiao-Jue Liu, and Ai-Ci Qiu. "Hybrid PCB Rogowski coil for measurement of nanosecond-risetime pulsed current." IEEE Transactions on Plasma Science 43, no. 10 (2015): 3555-3561. https://doi.org/10.1109/TPS.2015.2415517
[20] Han, Shejiao, Xutao Han, and Wei Sun. "The analysis of magnetic flux density inside Rogowski coil based on full current theory." IEEE Sensors Letters 4, no. 7 (2020): 1-4. https://doi.org/10.1109/lsens.2020.2987707
[21] Mor, A. Rodrigo, F. A. Muñoz, J. Wu, and LC Castro Heredia. "Automatic partial discharge recognition using the cross wavelet transform in high voltage cable joint measuring systems using two opposite polarity sensors." *International Journal of Electrical Power & Energy Systems* 117 (2020): 105695. https://doi.org/10.1016/j.ijepes.2019.105695
[22] Dey, D., B. Chatterjee, S. Chakravorti, and S. Munshi. "Cross-wavelet transform as a new paradigm for feature extraction from noisy partial discharge pulses." *IEEE Transactions on Dielectrics and Electrical Insulation* 17, no. 1 (2010): 157-166. https://doi.org/10.1109/TDEI.2010.5412014
[23] Naghashan, M. R., H. Zareie, and B. Anvarifar. "PD-source recognition in generator bars using a high-voltage coaxial-type high-pass filter." In *2007 Electrical Insulation Conference and Electrical Manufacturing Expo*, pp. 35-38. IEEE, 2007. https://doi.org/10.1109/eeic.2007.4562583
[24] Zhang, Guozhi, Changyue Lu, Xingyu Yu, Hanlv Tian, and Xiaoxing Zhang. "Research on Integrated Technology of PD Ultrasonic Signal and UHF Signal Detection." In *2022 IEEE International Conference on High Voltage Engineering and Applications (ICHVE)*, pp. 1-4. IEEE, 2022. https://doi.org/10.1109/ICHVE53725.2022.9961712
[25] Zhang, Xiaohua, Bo Pang, Yaxin Liu, Shaoyu Liu, Peng Xu, Yan Li, Yifan Liu, Leijie Qi, and Qing Xie. "Review on detection and analysis of partial discharge along power cables." Energies 14, no. 22 (2021): 7692. https://doi.org/10.3390/en14227692
[26] Radzi, MIF Mohamad, M. R. Ahmad, NH Nik Ali, and A. Mohd Ariffin. "Development of partial discharge detection device for PD detection on medium voltage XLPE cable." In *2020 8th International Conference on Intelligent and Advanced Systems (ICIAS)*, pp. 1-5. IEEE, 2021. https://doi.org/10.1109/ICIAS49414.2021.9642630
[27] Adhikari, Neha. "Studies on the Characteristics of Partial Discharges in High-Voltage XLPE Cable Joints exposed to Lightning Impulse Voltages." In 2023 Second International Conference on Electrical, Electronics, Information and Communication Technologies (ICEEICT), pp. 1-5. IEEE, 2023. https://doi.org/10.1109/ICEEICT56924.2023.10157592
[28] Wu, Ju-Zhuo, Jia-Jun Lin, Zi-Jian Gao, Hui-Hong Lin, Qin-Qiang Li, and Chen-Chen Zhang. "Removing white noise in partial discharge signal based on wavelet entropy and improved threshold function." In 2018 International Conference on Power System Technology (POWERCON), pp. 3924-3928. IEEE, 2018. https://doi.org/10.1109/POWERCON.2018.8602162
[29] Zhang, Zhen, Peng Fu, Ge Gao, Li Jiang, and Linsen Wang. "A Rogowski digital integrator with comb filter signal processing system." IEEE Transactions on Plasma Science 46, no. 5 (2018): 1338-1343. https://doi.org/10.1109/TPS.2018.2815699